V.V. MOKLYAK,[1] V.O. KOTSYUBYNSKY,[2] I.P. YAREMIY,[2] P.I. KOLKOVSKYY,[3]
A.B. HRUBYAK,[2] L.Z. ZBIHLEY[1]

[1] G.V. Kurdyumov Institute for Metal Physics, Nat. Acad. of Sci. of Ukraine
  (36, Vernadskyi Ave., Kyiv 03142, Ukraine; e-mail: mvvmcv@mail.ru)
[2] Vasyl Stefanyk Precarpathian National University
  (57, Shevchenko Str., Ivano-Frankivsk 76025, Ukraine)
[3] Joint Scientific and Research Laboratory of the Physics of Magnetic Films,
  G.V. Kurdyumov Institute for Metal Physics, Nat. Acad. of Sci. of Ukraine and
  Vasyl Stefanyk Precarpathian National University
  (57, Shevchenko Str., Ivano-Frankivsk 76025, Ukraine)

UDC 539

MORPHOLOGICAL CHARACTERISTICS OF HYDROTHERMALLY SYNTHESIZED IRON TRIFLUORIDES WITH VARIOUS HYDRATION DEGREES

The crystalline and magnetic microstructures and the morphological features of β-$FeF_3\,3H_2O$, HTB-$FeF_3\,0.33H_2O$, and r-FeF_3 iron fluorides hydrothermally synthesized and annealed in the argon atmosphere have been studied. The dehydration process of plate-like β-$FeF_3\,3H_2O$ particles is studied in detail, and the model for corresponding structural modifications is proposed. The developed model is used to synthesize ultradispersed HTB-$FeF_3\,0.33H_2O$ and r-FeF_3 materials. The r-FeF_3 phase is found to be partially in the superparamagnetic state, with the particle size being comparable with the average size of coherent scattering regions.

K e y w o r d s: iron trifluoride, dehydration, morphological properties, Mössbauer spectroscopy, thermogravimetric analysis, superparamagnetic state.

1. Introduction

Iron trifluoride r-FeF_3 is one of the most promising cathode materials. This fact is associated with the stability of its crystal structure owing to strong ionic bonds metal-ligand and a relatively high open-circuit voltage (up to 4 V with respect to Li^+/Li) at rather a small molar mass [1–4]. The maximum theoretical specific capacity of the substance amounts to 712 A h/kg. Iron trifluoride can be considered as a competitor to the market-dominating cathode material on the basis of $LiCoO_2$ and to another promising compound, $LiFePO_4$. At the same time, r-FeF_3 is an insulator with an energy gap width of 4.48 eV and rather a low conductivity [5, 6]. These properties are the main obstacle for its application in electrochemical current sources. The application of nanostructured materials and nanocomposites with conducting additives makes it possible to optimize the processes of charge transport in the electrode and partially solve this problem.

Iron fluorides with nano-sized particles are mainly synthesized, by using liquid-phase methods [7, 8]. At the same time, it is highly probable that the thermal dehydration of obtained hydrated products is accompanied by their pyrohydrolysis, which gives rise to the formation of the hematite phase [9]. In spite of a considerable interest in this problem, the dehydration of iron trifluoride crystalline hydrates remains to be rather poorly studied. Moreover, the literature sources give contradictory data on the temperature regimes required for a fabrication of water-

free r-FeF$_3$. The available fragmentary reports do not provide a complete picture of structural phase transformations occurring at the annealing of hydrated nanostructured iron trifluorides. This circumstance, in its turn, does not allow one to synthesize materials with required structural and morphological characteristics suitable for the application to the technology of lithium current sources. Therefore, the fabrication of iron trifluoride with nano-sized particles and various hydration degrees, as well as its water-free forms, together with the establishment of interrelations between the synthesis conditions and the morphological and structural features of obtained materials, composes an important scientific and practical problem. This work is devoted to its solution.

2. Experimental Technique

In order to produce the crystalline hydrate of iron trifluoride, FeF$_3$3H$_2$O, we combined the liquid-phase and hydrothermal methods. At the first stage, the 25% ammonia solution was introduced drop-by-drop into the 0.1M aqueous solution of Fe(NO$_3$)$_3$ under conditions of the intense stirring of the latter until the precipitate of iron hydroxide, Fe(OH)$_3$, appeared. The precipitate was held for 4 h, washed out with deionized water to $pH = 6.7$, and centrifugated. At the next stage, as-precipitated iron hydroxide, Fe(OH)$_3$, was dissolved in the 40% hydrofluoric acid to form [FeF$_6$]$^{3-}$ cation complexes. The obtained transparent and colorless solution was held in an autoclave for 10 h at a temperature of 70 °C. The solution was permanently stirred until a pink color appeared. Then the solution was evaporated in air at 80 °C to obtain a pink precipitate, FeF$_3$3H$_2$O. The remaining HF and water were removed by drying the precipitate in a vacuum furnace at a temperature of 80 °C for 12 h.

The phase composition and the crystal structure of synthesized materials were analyzed with the help of a diffractometer DRON-3.0 with the Bragg–Brentano focusing geometry of X-rays in the radiation emitted by a copper anode ($\alpha = 1.54178$ Å) and with a Ni filter. For studying the magnetic microstructure, the method of Mössbauer spectroscopy was used: an MS-1104Em device, the constant-acceleration regime, the Co^{57} isotope with an activity of 100 mCi in a chromium matrix serving as a source of γ quanta,
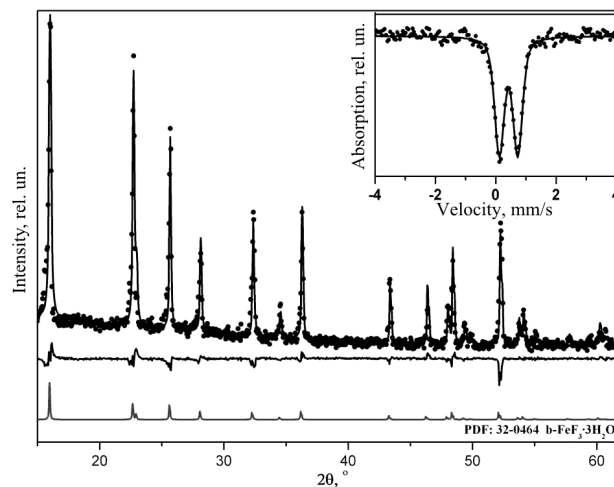

Fig. 1. Experimental diffraction patterns of the β-FeF$_3$3H$_2$O phase (points) and the results of its analysis by the Rietveld method (curve). The differential spectrum and the experimental diffraction pattern [10], which was included into the database PDF: 32-0464, are shown below. The Mössbauer spectrum of the material concerned is depicted in the inset

the line width of metallic α-Fe equal to 0.21 mm/s, and the calibration of isomeric shifts with respect to α-Fe.

Thermogravimetric researches were carried out on a thermal analyzer STA 499 F3 JUPITER in an argon flux of 0.4×10^{-7} m^3/s at a temperature variation rate of 5 °C/min in an interval of 20–600 °C. The structure-adsorption characteristics were determined by analyzing the isotherms of nitrogen sorption at the temperature $T = -195.75$ °C (77.4 K) on an automatic sorbometer Quantachrome Autosorb (Nova 2200e). The specimens were preliminarily degassed in a vacuum chamber with a residual pressure of 1.3 Pa at temperatures of 80–120 °C for 2 h. Morphological researches of the structure were carried out on a raster electron microscope JSM-6700F.

3. Results and Their Discussion

According to the results of X-ray phase analysis (XPA) and Mössbauer spectroscopy (Fig. 1), the produced material was the β-form of the crystalline hydrate of iron trifluoride (β-FeF$_3$3H$_2$O, PDF: 32-0464 [10]) with a modified crystallographic basis proposed by us in work [11] (see Table). In particular, the coordinates for F$^-$ and O^{2-} ions in (8g)-positions were
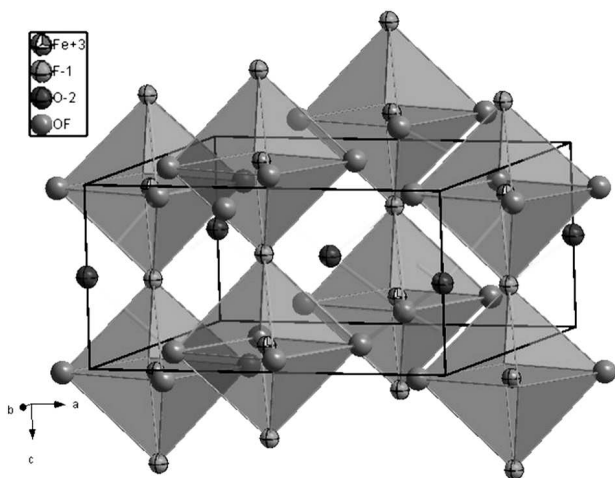
Fig. 2. Model of crystal structure for the β-FeF$_3$3H$_2$O phase

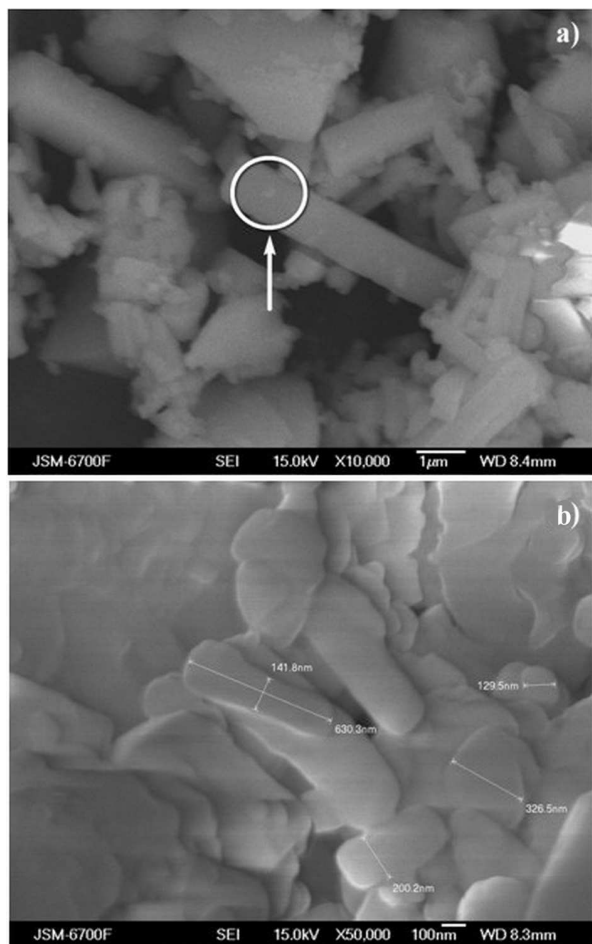**Fig. 3.** Microscopic images of the obtained β-FeF$_3$3H$_2$O material

changed from (0.2754, 0.1025, 0.1394) (coordinates were given in work [12], PDF: 85-0404, ICSD 14134) to (0.2754, 0.1025, 0.8794).

A satisfactory agreement between the experimental and calculated diffraction patterns was obtained, when we assumed the existence of such a texture, in which lamellar particles with the orientation in the (100) plane prevailed [13]. The general view of the crystalline structure of β-FeF$_3$3H$_2$O with the proposed crystallographic basis (Table) is illustrated in Fig. 2.

According to this model, [Fe(H$_2$O)$_2$F$_2$F$_2$] octahedra with the central cation Fe^{3+} are located in the plane with the prevailing (100) orientation of particles along the [001] direction of the crystallographic axis. Those octahedra form structural chains along the direction of their axial axes. For the connection, they use common F$^-$ anions located at the axial vertices of octahedra. The model is supported by the results of Mössbauer spectroscopy (Fig. 1), according to which there is only one type of octahedral positions for the localization of Fe^{57} nuclei in the material structure. The Mössbauer spectrum is formed by a single doublet component with the parameters $I_S = 0.42$ mm/s and $Q_S = 0.61$ mm/s, which unambiguously testifies that the material contains only Fe^{3+} ions in the close environment of the same type. As a result, the equiprobable filling of the equatorial plane of [Fe(H$_2$O)$_2$F$_2$F$_2$] octahedra by F$^-$ ions and H$_2$O molecules is observed. The chains of [Fe(H$_2$O)$_2$F$_2$F$_2$] octahedra in the structure of β-FeF$_3$3H$_2$O are separated by water molecules located at (2b)-positions. The latter form chains oriented along the crystallographic axis [001] and with a bond length of 3.8770 Å in between. On a micrograph (Fig. 3, a), one can clearly distinct prismatic blocks with average dimensions of about $1 \times 1 \times 5$ μm^3 and their separate fragments. The whole picture corre-

Basis parameters for the crystal structure (of the β-FeF$_3$H$_2$O phase (space group P4/nS, Fedorov group 85)

Atom	#	Ox.	Pos.	x	y	z	SOF	B
Fe	1	+3	2c	0	0.5	0.1453	1	1.29
F	1	−1	2c	0	0.5	0.6421	1	1.34
O	1	−2	2b	0	0	0.5	1	1.75
O	2	−2	8g	0.2754	0.1025	0.8794	0.5	2.08
F	2	−1	8g	0.2754	0.1025	0.8794	0.5	2.08

sponds to the tetragonal structure of the β-FeF$_3$3H$_2$O phase.

The obtained results agree with the data of works [14–16]. When producing the β-FeF$_3$3H$_2$O phase, the cited authors used the method of crystallization from the oversaturated solutions [14], hydrothermal method with the application of surfactants [15], and simple liquid-phase method [16]. They marked that the main macrostructural elements of the β-FeF$_3$3H$_2$O phase are micron-sized tetragonal blocks. However, in our case, as one can see from the scaled-up image of the surface of a separate block (Fig. 3, *b*), a lamellar structure is formed, with particles in the form of lamellae with average dimensions of 150×500 nm^2. This fact confirms our assumption that there is a texture in the (100) plane.

The formation of a lamellar structure is a result of the application of a hydrothermal treatment under the conditions, when the formation of a considerable number of nucleation centers in the whole volume of the solution is highly probable. As an evidence for this model, we may take the change of the solution color from colorless to pink owing to polycondensation processes and the formation of [Fe(H$_2$O)$_2$F$_2$F$_2$] octahedron chains. Under the acid-medium conditions, the hydrolysis degree of a reaction mixture is rather insignificant. Therefore, we may assert that there are almost no OH$^+$ groups in vicinities of iron ions, where water molecules dominate absolutely. As a result of the further evaporation, individual chains unite with one another – this process occurs owing to the van der Waals interaction between the H$_2$O molecules located on the lateral surfaces of chains in the near-surface region of the solution, where the intense evaporation takes place – and form particles with the lamellar morphology. Hence, it was the applied synthesis conditions that stimulated the prevailing direction of particle growth in the (100) plane.

In the course of further concentration of the solution with the help of the evaporation, the β-FeF$_3$3H$_2$O phase precipitates in the form of tetragonal prisms, which are agglomerates of lamellar particles. The corresponding size of coherent scattering regions (CSRs) was estimated with the help of the Williamson–Hall method on the basis of XPA data to equal about 42 nm, which gives a notion about the thickness of the plates in the direction of the crystallographic axis [001], as well as about their structure: the plates are agglomerates of separate CSRs in the
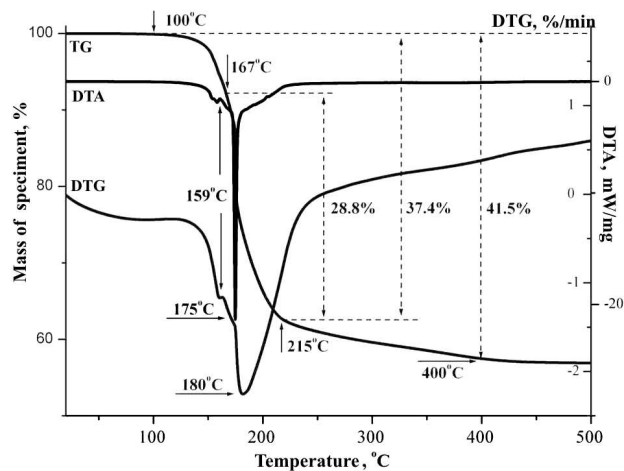

Fig. 4. TG, DTG, and DTA curves for the synthesized β-FeF$_3$3H$_2$O material

form of distorted cubes (with a shape close to the spherical one), which are united in the (100) plane into one or several layers.

To obtain information concerning the development of dehydration processes in the obtained β-FeF$_3$3H$_2$O phase with lamellar particles, thermogravimetric (TG) researches were carried out (Fig. 4). To prevent the pyrohydrolysis [9], we applied the annealing in the argon atmosphere. In comparison with thermogravimetric researches of commercial crystalline hydrate β-FeF$_3$3H$_2$O [11], the dehydration process began, in our case, at a temperature of 100 °C. More specifically, a shift of the temperature interval, in which the main mass fraction was lost (in our case, this was an interval from 100 to 215 °C) toward low temperatures by about 15 °C was detected (see the TG-curve in Fig. 4). Probably, this phenomenon is a result of the combined action of two factors. First, this is the size non-uniformity for both constituting particles and their agglomerates: the CSR size amounted to about 52 nm for the commercial material, and about 42 nm for that synthesized by us. In both cases, the material structure was created by packets of [Fe(H$_2$O)2F$_2$F$_2$] octahedra with water molecules localized in between. At the thermal treatment, the crystallites delaminated along the family of (110) planes, which was followed by the removal of some H$_2$O molecules from the as-formed surfaces in the course of transformation from the tetragonal structure into the orthorhombic one. The efficiency of this process was governed by the dimensions of crys-
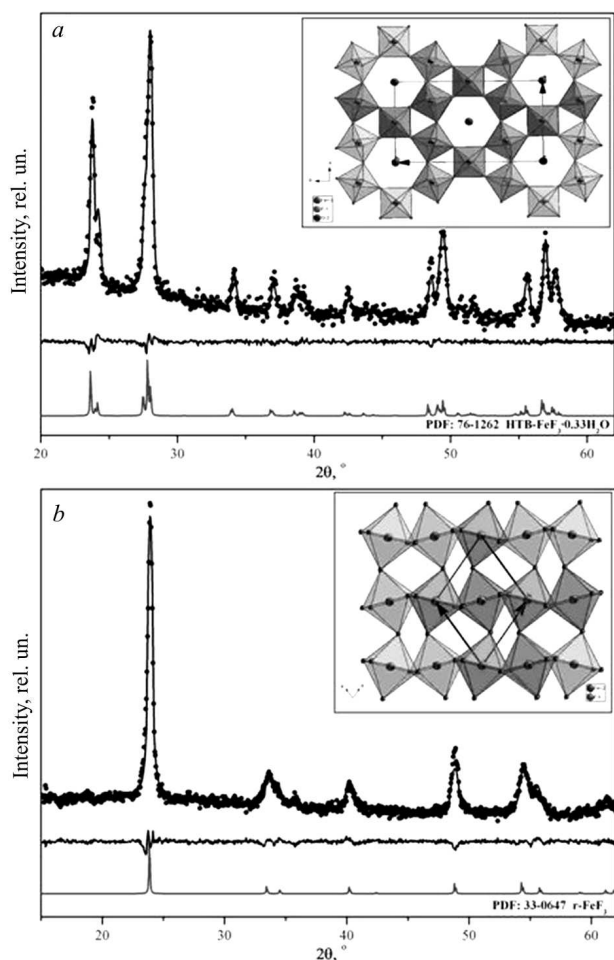
Fig. 5. Experimental diffraction patterns (points) and the results of their analysis using the Rietveld method (curves) for the β-FeF$_3$3H$_2$O (*a*) and r-FeF$_3$ (*b*) phases. The corresponding differential spectra and theoretical diffraction patterns are shown below. The insets illustrate the corresponding models of crystal structure

tallites. Second, the formation of agglomerates from particles with the lamellar morphology was observed in the synthesized material. Therefore, sorbed water molecules might remain located between separate plates. As a result, the dehydration region for the synthesized material shifted toward lower temperatures and was characterized by a complicated scenario of mass loss at this stage. The differential thermogravimetric (DTG) curve characterizing the rate of mass loss has a global maximum at 180 °C. In addition, the DTG and DTA (differential thermal analysis) curves reveal insignificant local minima in a vicinity of 159 °C, which may be associated, probably, with the removal of adsorbed OH$^-$ groups.

Hence, the dehydration of crystalline hydrate β-FeF$_3$3H$_2$O with lamellar particles is a multistage process. At the first stage, OH$^-$ groups are desorbed in a temperature interval of 100–162 °C, which is verified by the presence of an endo peak in the DTA curve at 159 °C and a change of the TG-curve slope in a vicinity of 162 °C. The corresponding mass loss amounts to 8.6%. The next stage includes the phase transition β-FeF$_3$3H$_2$O → HTB-FeF$_3$3H$_2$O with the removal of hydrated water (2.67 H$_2$O molecules per FeF$_3$3H$_2$O formula unit) in a temperature interval of 162–215 °C, which is verified by the presence of the main endo peak in the DTA curve in a vicinity of 175 °C [11] and the correspondence of the measured mass loss of the specimen to a theoretically calculated value of 28.8% (crystalline hydrate HTB-FeF$_3$0.33H$_2$O has *Cmcm* space group symmetry [17]). The third stage includes the phase transition HTB-FeF$_3$0.33H$_2$O → HTB-FeF$_3$ followed by the removal of hydrated water in a temperature interval of 215–460 °C. At this stage, no variations in the crystal structure and its parameters take place [18]. In this temperature interval, no changes were fixed in the DTA curve, but a change in the TG-curve slope was observed in a vicinity of 400 °C. A gradual reduction of the mass loss rate was detected in a temperature interval of 215–460 °C. The mass loss itself at this stage amounted to about 4%, which corresponds to the theoretically calculated value. The HTB-FeF$_3$ phase was metastable and irreversibly transformed into rhombohedral r-FeF$_3$ (*R-3cR* space group symmetry), with no specimen mass being lost at that. The further heating of the specimen to 600 °C did not change its structure and mass.

The results of thermogravimetric analysis obtained for the development of the dehydration process of β-FeF$_3$3H$_3$O formed a basis for the selection of a strategy for producing FeF$_3$0.33H$_2$O and FeF$_3$. The former was obtained by applying the thermal annealing in the argon atmosphere at a temperature of 180 °C for 4 h. For producing the latter, the initial crystalline hydrate was thermally annealed in the argon flux (a rate of gas supply of 42×10^{-9} m^3/s) at a temperature of 400 °C for 4 h. In our case, the holding time was increased to 4 h in comparison with the dehydration procedure applied in work [11] in order to

provide the monophase character of the decomposition end-products. As a result, according to the XPA data (Fig. 5), we obtained the following monophase materials: HTB-FeF$_3$0.33H$_2$O with the structure of hexagonal tungsten bronze (PDF: 76-1262) and the rhombohedral modification of iron trifluoride, r-FeF$_3$ (PDF: 33-0647).

The average CSR sizes were estimated within the Williamson–Hall method. For the mentioned phases, they amounted to 26 (HTB-FeF$_3$0,33H$_2$O) and 23 nm (r-FeF$_3$). According to the Mössbauer spectroscopy data (Fig. 6), the structure of the obtained HTB-FeF$_3$0,33H$_2$O phase was characterized by only one type of octahedral positions for the localization of Fe^{57} nuclei, because the Mössbauer spectrum was formed by a single doublet component with the parameters I_S = 0.42 mm/s and Q_S = 0.59 mm/s (Fig. 6, a). At the same time, the Mössbauer spectrum of the r-FeF$_3$ specimen (Fig. 6, b) was a superposition of a Zeeman sextet and two doublet components. The sextet with the parameters I_S = 0.46 mm/s, Q_S = 0.05 mm/s, and H = 399 kOe and the major doublet component were formed as a result of the resonant absorption of γ-quanta by Fe^{57} nuclei that entered the r-FeF$_3$ particles. The latter were in either a magnetically ordered (72%) or a superparamagnetic (25%) state.

It is worth noting that the magnitude of quadrupole splitting for the dominant doublet component (Q_S = 0.64 mm/s) differs from the result of work [11], where the value Q_S = 0.12 mm/s was registered. The value of quadrupole splitting close to zero agrees well with the crystallographic model, in which the near environment of every Fe^{3+} ion – it is formed by F$^-$ anions – is spherically symmetric. The observed changes are associated with morphological features of the material composed of particles with a pronounced prismatic shape (Fig. 7, c). At the same time, these blocks are agglomerates of particles with an average size of about 20–30 nm (Fig. 7, d).

Thus, the following model can be developed for the structural transformations occurring at the dehydration of the β-FeF$_3$3H$_2$O phase (Fig. 8). In the course of heating, after the removal of adsorbed OH$^-$ groups, the specimen starts to lose hydrated water. First of all, H$_2$O molecules escape from some of (2b) structural positions in β-FeF$_3$3H$_2$O. As a result,

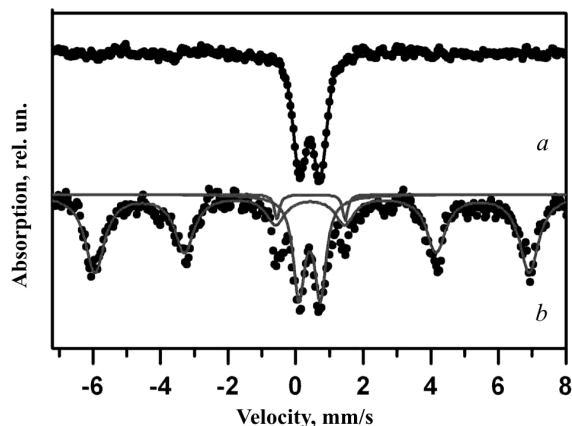***Fig. 6.*** Mössbauer spectra of HTB-FeF$_3$0.33H$_2$O (a) and r-FeF$_3$ (b)

the tetragonal blocks inherent to this phase crack along the [001] crystallographic axis and the family of (110) planes (Fig. 8) to form prismatic blocks. The further removal of H$_2$O molecules entering the composition of [Fe(H$_2$O)$_2$F$_2$F$_2$] octahedra from the (8g) structural positions, stimulates the phase transition β-FeF$_3$3H$_2$O $\rightarrow$ HTB-FeF$_3$0.33H$_2$O. As a result, the crystal lattice transforms from tetragonal into orthorhombic. This process is accompanied by the formation of [FeF$_6$] octahedra. The latter join with one another by means of four common vertices and form hexagonal channels filled with molecules of structurally bound water in the HTB-FeF$_3$0.33H$_2$O structure. After all those processes have terminated, the annealing of the specimen in an inert atmosphere at a temperature of 180 °C for 4 h gives rise to the formation of structural blocks of the HTB-FeF$_3$0.33H$_2$O phase of the "corn-cob" type (Fig. 8). The blocks are agglomerates of particles which look like hexagonal prisms elongated along the crystallographic axis [001] and with a lateral face width of about 200 nm. In this case, the formation of a fine grain structure (Fig. 7, b) marks the beginning of the next dehydration stage: the removal of water molecules from the (4c) structural positions in the HTB-FeF$_3$0.33H$_2$O phase. As a result, the hexagonal rods become separated into grains perpendicularly to their axial axes. The average CSR size in this phase amounts to about 26 nm.

When the temperature increases to 400 °C, the phase transition HTB-FeF$_3$0.33H$_2$O $\rightarrow$ r-FeF$_3$ takes place. It is acompanied by the transformation of the
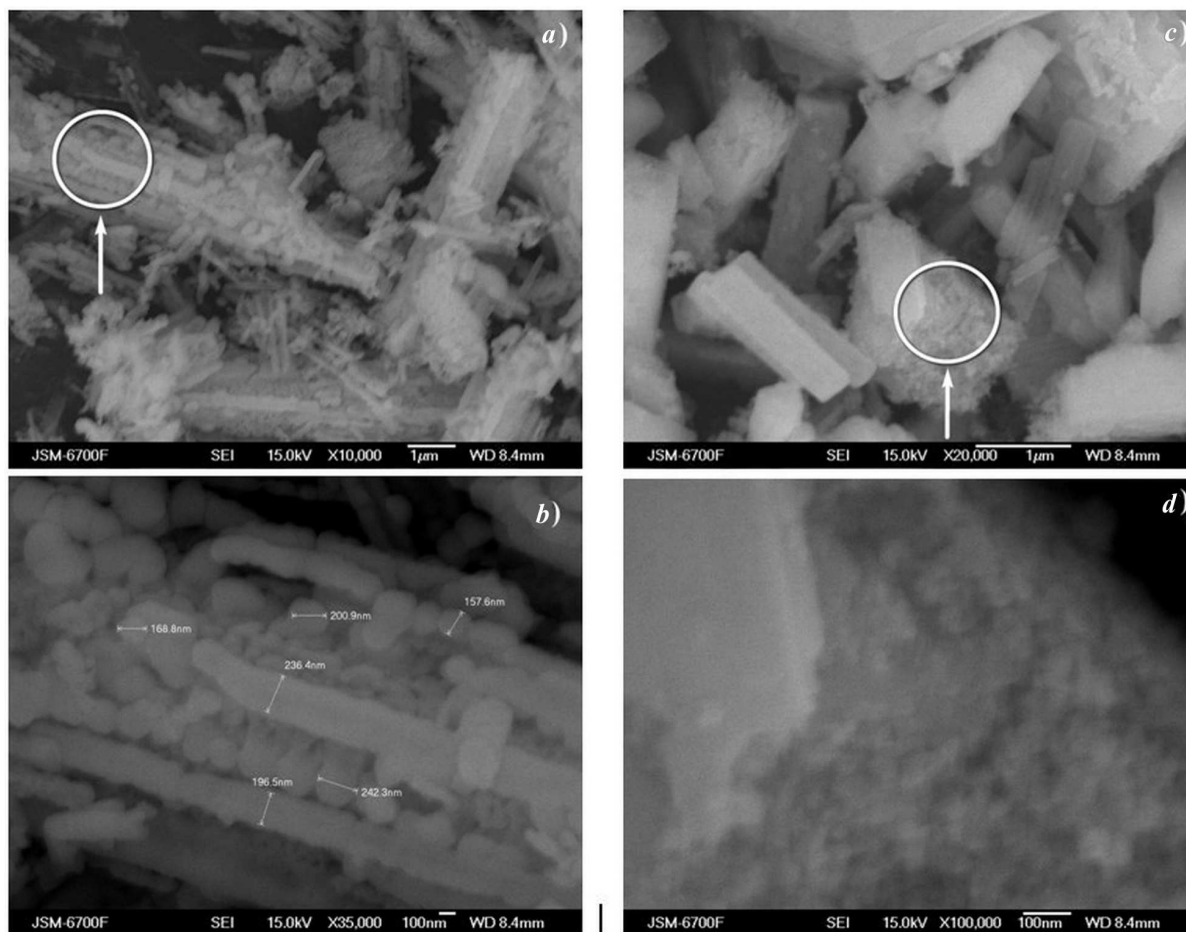
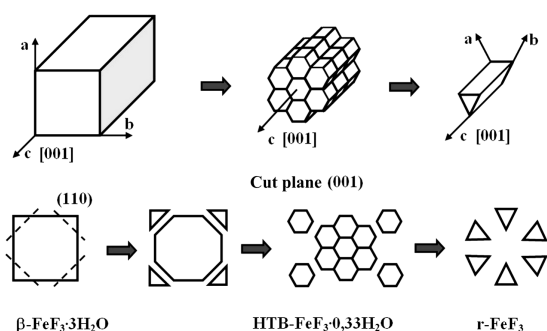**Fig. 7.** Microscopic images of the obtained materials: HTB-FeF$_3$0.33H$_2$O (*a* and *b*) and r-FeF$_3$ (*c* and *d*)

Fig. 8. Model of structural transformations at the dehydration of the obtained material β-FeF$_3$3H$_2$O

crystal lattice from orthorhombic into rhombohedral. The structural blocks of the "corn-cob" type inherent to the HTB-FeF$_3$0.33H$_2$O phase become destroyed: the particles of this phase in the form of

hexagonal prisms crack further along the crystallographic axis [001] and form blocks of the r-FeF$_3$ phase. These blocks are trihedral prisms (Fig. 8), and they are agglomerates of particles with an average size of about 20–30 nm (Fig. 7, *d*), which are characterized by the presence of a surface "crust". In this case, the size of constituting particles is comparable with the average size of CSR in this phase (23 nm). This conclusion is confirmed by the results of Mössbauer spectroscopy, according to which 25 wt.% of the material are in the superparamagnetic state, which assumes that there should exist particles with dimensions less than 16 nm [11].

Our conclusions about the particle dispersion in the obtained materials during their dehydration agree with results of the adsorption porometry. In particular, the specific surface areas for the β-FeF$_3$3H$_2$O,

HTB-FeF$_3$0.33H$_2$O, and r-FeF$_3$ phases amount to 2, 10, and 50 m^2/g, respectively. As an additional confirmation, we may consider the established minor doublet component (with a relative content of about 3%) in the Mössbauer spectrum of the r-FeF$_3$ phase. The parameters of this component, $I_S = 0.45$ mm/s and $Q_S = 2.02$ mm/s, mean that it appears owing to the resonant absorption by the nuclei of iron ions in a state that is intermediate between the Fe^{2+} and Fe^{3+} ones, which testifies to a substantially developed surface of the specimen.

4. Conclusions

To summarize, the hydrothermal synthesis and the following thermal annealing were applied to obtain β-FeF$_3$3H$_2$O, HTB-FeF$_3$0.33H$_2$O, and r-FeF$_3$ monophases, in which particles possess the morphology of tetragonal prisms, are blocks of the "corncob" type, and look like trihedral prisms, respectively. The constituting particles in the β-FeF$_3$3H$_2$O phase have a lamellar morphology and are characterized by average dimensions of 150×500 nm^2. At the same time, the particles in the HTB-FeF$_3$0.33H$_2$O phase have a morphology of hexagonal prisms elongated along the crystallographic axis [001] and with a lateral face width of about 200 nm. The average sizes of CSRs in those phases amount to 42 and 26 nm, respectively.

The main structural blocks of the r-FeF$_3$ phase are trihedral prisms with a surface "crust". Beneath the crust, there are agglomerated constituting particles, whose size is comparable with the average size of CSR in this phase (23 nm). About 25% of the material are in the superparamagnetic state.

A model has been proposed for those structural transformations that accompany the dehydration process of crystalline hydrate β-FeF$_3$3H$_2$O. It is shown that the sequence of phase transitions β-FeF$_3$3H$_2$O $\rightarrow$ HTB-FeF$_3$0.33H$_2$O $\rightarrow$ r-FeF$_3$ gives rise to the removal of H$_2$O molecules from the structural positions (2b) and (8g) in the β-FeF$_3$3H$_2$O phase and the (4c) position in the HTB-FeF$_3$0.33H$_2$O phase, which is accompanied by the destruction of prismatic particles in those phases along their crystallographic axis [001]. As a result, a decrease of the particle size and an increase of the specific surface area in the end-product (the FeF$_3$ phase) to a value of 50 m$_2$/g were observed.

1. F. Wang, R. Robert, N.A. Chernova *et al.* Conversion reaction mechanisms in lithium ion batteries: Study of the binary metal fluoride electrodes. *J. Am. Chem. Soc.* **133**, 18828 (2011) [DOI: 10.1021/ja206268a].
2. Y. Makimura, A. Rougier, J.M. Tarascon. Pulsed laser deposited iron fluoride thin films for lithium-ion batteries. *Appl. Surf. Sci.* **252**, 4587 (2006) [DOI 10.1016/j.apsusc.2005.06.043].
3. S.W. Kim, D.H. Seo, H. Gwon *et al.* Fabrication of FeF$_3$ nanoflowers on CNT branches and their application to high power lithium rechargeable batteries. *Adv. Mater.* **22**, 5260 (2010) [DOI: 10.1002/adma.201002879].
4. H. Jung, H. Song, T. Kim *et al.* FeF$_3$ microspheres anchored on reduced graphene oxide as a high performance cathode material for lithium ion batteries. *J. Alloys Compd.* **647**, 750 (2015) [DOI: 10.1016/j.jallcom.2015.06.191].
5. Z. Yang, Y. Pei, X. Wang *et al.* First principles study on the structural, magnetic and electronic properties of Co-doped FeF$_3$. *J. Comput. Theor. Nanosci.* **9**, 44 (2012) [DOI: 10.1016/j.comptc.2011.11.008].
6. Y. Kim, S. Choi, S. Kim. Investigation of the change in the electronic properties of FeF$_3$ by the introduction of oxygen using a molecular orbital method. *Int. J. Quant. Chem.* **114**, 340 (2014) [DOI: 10.1002/qua.24566].
7. J. Liu, W. Liu, S. Ji *et al.* Iron fluoride hollow porous microspheres: Facile solution-phase synthesis and their application for Li-ion battery cathodes. *Chem. Eur. J.* **20**, 5815 (2014) [DOI: 10.1002/chem.201304713].
8. Q. Chu, Z. Xing, J. Tian, X. Ren, A.M. Asiri, A.O. Al-Youbi, X. Sun. Facile preparation of porous FeF$_3$ nanospheres as cathode materials for rechargeable lithium-ion batteries. *J. Power Sources* **236**, 188 (2013) [DOI: 10.1016/j.jpowsour.2013.02.026].
9. E.G. Rakov, V.V. Teslenko. *Pyrohydrolysis of Inorganic Fluorides* (Energoatomizdat, 1987) (in Russian).
10. M.C. Morris, F.H. McMurdie, H. Eloise, B. Paretzkin. *Standard X-ray Diffraction Powder Patterns* (Nat. Bur. Standards, 1980).
11. V.V. Moklyak, V.A. Kotsyubynskyi, P.I. Kolkovskyy, A.B. Hrubyak, L.Z. Zbihley. Thermoinduced decomposition of hydrated iron trifluoride in an argon flow. *Metallofiz. Noveish. Tekhnol.* **37**, 355 (2015).
12. G. Teufer. The crystal structure of tetragonal ZrO$_2$. *Acta Cryst.* **15**, 1187 (1962).
13. H. Toraya, F. Marumo. Preferred orientation correction in powder pattern fitting. *Mineral. J.* **10**, 211 (1981).
14. K.M. Forsberg, C. Rasmuson. Crystallization of metal fluoride hydrates from mixed hydrofluoric and nitric acid solutions, part II: Iron (III) and nickel (II). *J. Cryst. Growth* **312**, 2358 (2010) [DOI: 10.1016/j.jcrysgro.2010.05.017].
15. J. Tan, L. Liu, H. Hu, Z. Yang, H. Guo, Q. Wei, H. Shu. Iron fluoride with excellent cycle performance synthesized by solvothermal method as cathodes for lithium ion batteries. *J. Power Sources* **251**, 75 (2014) [DOI: 10.1016/j.jpowsour.2013.11.004].

16. Li Liu, G. Haipeng, Z. Meng, W. Qiliang, Y. Zhenhua, S. Hongbo, Y. Xiukang, Y. Zichao, T. Jinlin, W. Xianyou. A comparison among $FeF_3 \cdot 3H_2O$, $FeF_3 \cdot 0.33H_2O$, and FeF_3 cathode materials for lithium ion batteries: Structural, electrochemical, and mechanism studies. *J. Power Sources* **238**, 501 (2013) [DOI: 10.1016/j.jpowsour.2013.04.077].

17. S.T. Myung, S. Sakurada, H. Yashiro, Y.K. Sun. Iron trifluoride synthesized via evaporation method and its application to rechargeable lithium batteries. *J. Power Sources* **223**, 1 (2013) [DOI: 10.1016/j.jpowsour.2012.09.027].

18. N. Louvain, A. Fakhry, P. Bonnet, M. El-Ghozzi, K. Guerin, M.T. Sougrati, J.C. Jumas, P. Willmann. One-shot *versus* stepwise gas–solid synthesis of iron trifluoride: Investigation of pure molecular F_2 fluorination of chloride precursors. *Cryst. Eng. Commun.* **15**, 3664 (2013) [DOI: 10.1039/C3CE27033E].

В.В. Мокляк, В.О. Коцюбинський,
І.П. Яремій, П.І. Колковський, А.Б. Груб'як, Л.З. Збіглей

МОРФОЛОГІЧНІ ХАРАКТЕРИСТИКИ
ТРИФТОРИДІВ ЗАЛІЗА РІЗНОГО СТУПЕНЯ
ГІДРАТАЦІЇ, ОТРИМАНИХ
ГІДРОТЕРМАЛЬНИМ МЕТОДОМ

Р е з ю м е

В роботі проведено дослідження кристалічної і магнітної мікроструктур та морфологічних особливостей матеріалів β-$FeF_3 \cdot 3H_2O$, HTB-$FeF_3 \cdot 0{,}33H_2O$ та r-FeF_3, отриманих гідротермальним методом з наступним відпалом в атмосфері аргону. Детально вивчено процес дегідратації кристалогідрату β-$FeF_3 \cdot 3H_2O$ з частинками пластинчастої форми та запропоновано модель структурних перетворень. Застосовуючи отримані узагальнення, синтезовано ультрадисперсні HTB-$FeF_3 \cdot 0{,}33H_2O$ та r-FeF_3. Встановлено, що фаза r-FeF_3 частково перебуває в суперпарамагнітному стані, при цьому розмір частинок матеріалу співмірний із середніми розмірами областей когерентного розсіювання.